

Fundamental Performance Limits for PLC Systems Impaired by Impulse Noise

Riccardo Pighi, Michele Franceschini, Gianluigi Ferrari and Riccardo Raheli,
 Dept. of Information Engineering, University of Parma, 43100 Parma, Italy
 Email: {pighi,mfrance,gferrari}@tlc.unipr.it, raheli@unipr.it

Abstract—In this paper, we provide insights on the ultimate performance limits, in terms of achievable information rate, for power line communication (PLC) systems impaired by *impulse noise*. In particular, we analyze single carrier (SC) and multiple carrier (MC) transmission systems employing quadrature amplitude modulation (QAM) formats. In order to compute the information rates of standard MC systems, we introduce a theoretically equivalent channel model which allows the *exact* computation of the information rate. This simplified channel model will be referred to as *interleaved MC channel* model. We show that the use of MC schemes leads to an unavoidable loss with respect to SC schemes. In order to validate our theoretical results, we analyze the bit error rate (BER) performance of SC and MC schemes through Monte Carlo simulations. Several trellis-coded modulation (TCM) and low-density parity-check (LDPC)-coded schemes are considered.

I. INTRODUCTION

In the last years, there has been a growing interest towards the use of existing power line communication (PLC) channels as an effective means for transmitting data and voice [1], [2]. One of the main noise types affecting PLC systems is the *impulse noise*, and the focus of this work is on the impact of this noise on the performance of PLC systems. We assume that the impulse noise is modeled as a Bernoulli-Gaussian process [3], i.e., the product of a Bernoulli process and a complex Gaussian process. However, the proposed approach can be straightforwardly extended to other impulse noise channel models.

The structure of this paper is the following. In the first part of this paper, the theoretical performance limits of the considered schemes are studied through computation and comparison of their mutual information [4], referred to as *information rate*. Three different types of channels are considered as representative of PLCs: (i) additive white Gaussian noise (AWGN) channel, (ii) Bernoulli impulse noise channel (where the impulse noise is modeled as a Bernoulli-Gaussian process [3]) and (iii) the *interleaved Bernoulli multicarrier* (MC) channel. The latter model is theoretical and allows to evaluate the information rate of standard MC systems, i.e., orthogonal frequency division multiplexing (OFDM) with forward error correction codes spread over the carriers. The theoretical results show that while the introduction of additive impulse noise in a single carrier (SC) scheme with AWGN leads to negligible information rate loss, the impact of impulse noise on standard MC schemes is deleterious.

In the second part of this paper, we validate the information-theoretic results through a bit error rate (BER) performance

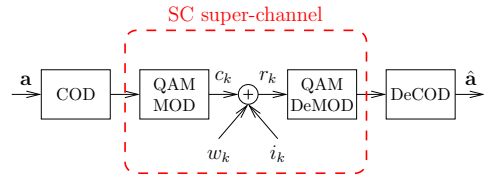


Fig. 1. SC communication system with AWGN and impulse noise.

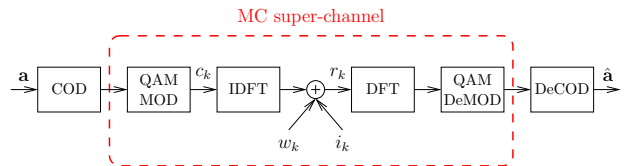


Fig. 2. MC communication system with AWGN and impulse noise.

analysis, based on Monte Carlo simulations, of several transmission schemes, both SC and MC. In particular, we consider: (i) trellis coded modulation (TCM) schemes [5] and (ii) a low-density parity-check (LDPC) coded scheme [6], both employing quadrature amplitude modulation (QAM) formats. The BER performance analysis is in good agreement with the information rate-based analysis. Finally, we show that the penalty which affects MC systems can be reduced using standard coding schemes complemented by suitable signal processing algorithms. We point out that the general conclusions derived on the impact of impulse noise hold regardless of the specific distribution of this noise.

II. SYSTEM AND CHANNEL MODELS

Evaluation of the information rate of SC schemes is well established [4]. However, computing the information rate of MC schemes is a complicated computational problem. Since the MC modulation and demodulation blocks correspond to invertible vector functions (inverse discrete Fourier transform, IDFT, and discrete Fourier transform, DFT), the use of MC schemes does not modify the capacity of the overall *super-channel*, including, together with the AWGN channel and the impulse noise, the QAM modulator and demodulator [4]. The superchannels in SC and MC schemes are shown in Fig. 1 and Fig. 2, respectively. Since MC codes are obtained by spreading an SC code, such as TCM [5] or LDPC [6], over the carriers, the system performance of MC schemes remains unchanged by considering the presence of an *ideal random interleaver* between the QAM modulator and the MC block. We refer to this theoretical scheme as *interleaved MC channel*.

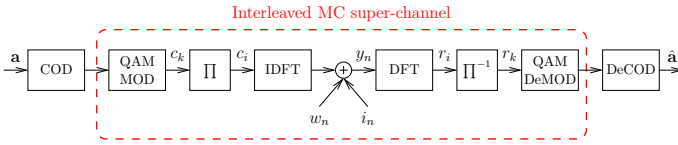


Fig. 3. *Interleaved MC communication system* (the ideal random interleaver is denoted as Π) with AWGN and impulse noise.

The key property of this scheme is that the superchannel becomes memoryless, and this leads to a feasible and *exact* computation of the information rate of the system. We point out that, while the interleaved MC channel model is expedient for the information-theoretic computations, in Section IV, this model will be used to derive “practical” detection algorithms.

A. SC Scheme with Bernoulli Impulse Noise

This scheme is shown in Fig. 1. The discrete time observable at the output of a channel with AWGN and impulse noise can be expressed as follows:¹

$$r_k = c_k + i_k + w_k \quad (1)$$

where c_k is a coded symbol belonging to a QAM constellation, w_k is a sample of AWGN with zero mean and unilateral power spectral density σ_w , and the impulse noise sample i_k can be written as [3] $i_k = b_k g_k$, where b_k is a Bernoulli random variable with parameter p and g_k is a complex white Gaussian random variable with zero mean and variance σ_i^2 . All of the above random variables are assumed independent. The probability density function (PDF) of the total channel noise $m_k \triangleq w_k + i_k$, denoted as $p(m)$, can be expressed as a mixture of Gaussian PDFs:

$$p(m) = (1-p)\mathcal{N}(m; 0, \sigma_w^2) + p\mathcal{N}(m; 0, \sigma_w^2 + \sigma_i^2) \quad (2)$$

where $\mathcal{N}(m; \eta, \sigma^2) \triangleq (1/2\pi\sigma^2) \exp\{-|m - \eta|^2/2\sigma^2\}$.

B. Interleaved MC Scheme with Bernoulli Impulse Noise

The interleaved MC scheme with Bernoulli impulse noise is depicted in Fig. 3. We now characterize the input-output relationship of the interleaved MC super-channel, shown in Fig. 3, comprising the IDFT block, the channel with AWGN and impulse noise, and the DFT block. The effects of the ideal interleaver will be analyzed afterwards.

The observable at the output of the Bernoulli channel can be described by the following

$$y_n = \frac{1}{\sqrt{N}} \sum_{i=0}^{N-1} c_i e^{j2\pi ni/N} + i_n + w_n \quad n = 0, \dots, N-1$$

where $\{c_i\}$ is the interleaved QAM coded symbol, w_n is a sample of AWGN, and i_n is the Bernoulli impulse noise sample defined in (1). The observable at the output of the DFT demodulation block can be written as follows:

$$r_i = \text{DFT}\{y_n\} = \frac{1}{\sqrt{N}} \sum_{n=0}^{N-1} y_n e^{-j2\pi ni/N} = c_i + W_i + I_i$$

¹In this paper, we assume an information lossless discretization of the received signal, i.e., the channel output.

where the third equality is due to the linearity of the DFT, W_i is a sample of the DFT of $\{w_n\}$, i.e., an AWGN sample with variance σ_w^2 per components, and I_i is defined as the DFT of $\{i_n\}$, i.e.:

$$I_i \triangleq \frac{1}{\sqrt{N}} \sum_{n=0}^{N-1} i_n e^{-j2\pi ni/N} \quad i = 0, \dots, N-1.$$

The PDF of the total noise sample at the output of the DFT, i.e., $M_i = W_i + I_i$, can be expressed as [3]

$$p(M) = \sum_{\ell=0}^N \binom{N}{\ell} p^\ell (1-p)^{N-\ell} \mathcal{N}(M; 0, \sigma_M^2[\ell]) \quad (3)$$

where

$$\sigma_M^2[\ell] \triangleq \sigma_w^2 + \ell \frac{\sigma_i^2}{N}. \quad (4)$$

As observed in the previous section, we ideally assume that an ideal random interleaver is inserted between the QAM modulator and the IDFT block and the corresponding ideal deinterleaver is inserted between the DFT block and the QAM demodulator at the receiver. As a consequence, the discrete time observable at the output of this channel model can be defined as

$$r_k = c_k + M_k.$$

The above assumption allows one to conclude that each time-consecutive QAM coded symbol is affected, at the receiver, by independent and identically distributed (i.i.d.) noise samples $\{M_k\}$, i.e., the channel is *memoryless*. Consequently, it is feasible to obtain *exact* information-theoretic results and *practical* detection algorithms.

III. INFORMATION-THEORETIC PERFORMANCE ANALYSIS: INFORMATION RATE

The mutual information rate between the sequence of uncoded input symbols $\{a_k\}$ and the output sequence $\{r_k\}$ of a channel can generally be written as

$$I(A; R) = h(R) - h(R|A) \quad (5)$$

where $h(R)$ and $h(R|A)$ are the differential and conditional differential entropy rates of the sequence $\{r_k\}$, respectively. Since the asymptotic equipartition property (AEP) holds [4], it is possible to evaluate $h(R)$ and $h(R|A)$ using a reasonably long information sequence, by means of Monte Carlo simulation techniques. In order to compute $h(R)$ and $h(R|A)$ in (5), we can express these two terms as follows:

$$\begin{aligned} h(R) &= \lim_{n \rightarrow \infty} \frac{1}{n} h(\mathbf{r}_0^n) = - \lim_{n \rightarrow \infty} \frac{1}{n} \mathbb{E} [\log(p(\mathbf{r}_0^n))] \\ &= - \lim_{n \rightarrow \infty} \frac{1}{n} \log [p(\mathbf{r}_0^n)] = - \lim_{n \rightarrow \infty} \frac{1}{n} \sum_{i=0}^n \log(p(r_i)) \quad (6) \\ h(R|A) &= \lim_{n \rightarrow \infty} \frac{1}{n} h(\mathbf{r}_0^n | \mathbf{a}_0^n) = - \lim_{n \rightarrow \infty} \frac{1}{n} \mathbb{E} [\log(p(\mathbf{r}_0^n | \mathbf{a}_0^n))] \\ &= - \lim_{n \rightarrow \infty} \frac{1}{n} \log [p(\mathbf{r}_0^n | \mathbf{a}_0^n)] = - \lim_{n \rightarrow \infty} \frac{1}{n} \sum_{i=0}^n \log(p(r_i | a_i)) \quad (7) \end{aligned}$$

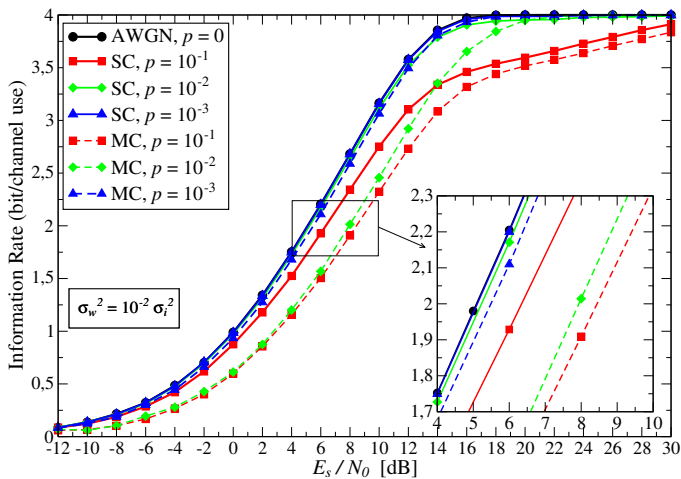


Fig. 4. Information rate for 16 QAM schemes, both SC and interleaved MC, with impulse noise. In each case, various values of the parameter p of the Bernoulli distribution for the impulse noise are considered. The variances of the impulse noise is $\sigma_w^2 = 10^{-2} \sigma_i^2$.

where $\mathbf{r}_{k_1}^{k_2}(\mathbf{a}_{k_1}^{k_2})$ is a shorthand notation for the vector collecting signal observations (information symbols) from time epoch k_1 to k_2 and $h(\mathbf{r}_0^n)$ ($h(\mathbf{r}_0^n|\mathbf{a}_0^n)$) is the differential entropy rate of the sequence \mathbf{r}_0^n (the conditional differential entropy rate). Given the memoryless nature of the noises, the generic PDF $p(r_i)$ in (6) and the generic conditional PDF $p(r_i|a_i)$ embedded in (7) can be easily expressed using (2) and (3), respectively. However, our analysis can also be extended to channels with memory! [7].

A. Numerical Results

In Fig. 4, the achievable information rates of SC and interleaved MC schemes with Bernoulli impulse noise are shown in the case with 16 QAM modulation format. We assume, in the remainder of this paper, that input information symbols are equiprobable. For the interleaved MC channel, the number of sub-channels is set to $N = 64$. The information rates are shown as a function of the signal-to-noise ratio (SNR) E_s/N_0 , where E_s is the received symbol energy. The Bernoulli parameter p takes on values in the representative set $\{10^{-1}, 10^{-2}, 10^{-3}\}$. We assume that the variance of the impulse noise is such that $\sigma_w^2 = 10^{-2} \sigma_i^2$ (i.e., the average power of the impulse noise is equal to that of the AWGN only when $p = 10^{-2}$). The computation of information rates has been carried out using Monte Carlo simulations in order to evaluate the limits in (6) and (7) [7]. The number of transmitted symbols is set to 10^7 , which guarantees good numerical accuracy. As one can observe from the results in Fig. 4, in a scenario with $p = 10^{-1}$, the behavior of the information rate for both SC and interleaved MC schemes differs from the other cases. More precisely, once the information rate curve reaches a critical value (in terms of bit/channel use), the slope of the curves reduces significantly and the information rate increases almost linearly. In other words, in the presence of strong impulse noise, the SNR required to achieve the theoretical maximum possible channel utilization (i.e., an information rate close to 4 bit/channel

use) is significantly higher than in a scenario where impulse noise and AWGN have the same weight. Observe also that the critical value of the channel utilization where the information rate slope changes is approximately equal to $4(1-p)$, for $p = 10^{-1}$. This is intuitively correct, since a high channel utilization corresponds to a scenario where the impulse noise has the strongest impact.

B. Discussion

We now comment on the obtained results, distinguishing between SC and interleaved MC schemes.

1) *SC Schemes*: From the results in Fig. 4, it is clear that, even if the impulse noise power equals the AWGN power, the impact of the impulse noise on the achievable information rate of SC schemes is negligible, as long as the impulse noise event occurs rarely enough (i.e., p is sufficiently small). Thus, a properly designed transmission system operating on an impulse noise environment should perform “just as if there were no impulse noise.”

2) *Interleaved MC Schemes*: The information-theoretic results, associated with interleaved MC systems, presented in Fig. 4, are obtained inserting a (theoretical) ideal infinite interleaver. These performance results suggest that MC systems, designed assuming the independence of the noise samples affecting different sub-carriers, should exhibit a significant penalty (about 3 dB, with the considered noise model parameters), with respect to a single AWGN channel. The penalty affecting MC systems has, therefore, a different nature with respect to the penalty affecting SC systems. In the SC case, the penalty is intrinsic, i.e., it is caused by the introduction of the impulse noise, and no coding scheme nor proper modulation design can overcome it. In the MC case, the penalty is due to the system design constraint, i.e., the transmission of a coded QAM sequence for a memoryless channel spread over the sub-carriers. As opposed to the penalty affecting SC systems, this one can be recovered by proper coding/modulation and detection design.

IV. COMMUNICATION-THEORETIC PERFORMANCE ANALYSIS: BIT ERROR RATE

In order to validate the prediction of our information-theoretic analysis, we now evaluate, through Monte Carlo simulations, the performance of several SC and MC *coded* schemes, in terms of their BER.

A. Trellis Coded Modulated Transmission

TCM is a widely used coding/modulation technique for spectrally efficient communication systems [5]. In this subsection we describe its application to communication schemes with impulse noise. We first introduce the exact branch metric to be used in a Viterbi algorithm (VA) in order to perform maximum *a posteriori* (MAP) sequence detection in an SC scheme with Bernoulli-Gaussian impulse noise. Then, we compute the branch metric to be used in the VA for an interleaved MC system where the PDF of the total noise at the output is given by (3), assuming independent noise samples. Finally,

we present numerical results to characterize the performance of TCM schemes. We compare the BER curves of an MC TCM system with the Euclidean metric and the exact branch metric for the Bernoulli-Gaussian noise process, respectively. We also consider an MC system using a very simple *time-domain processing*, suggested by the information-theoretic results.

1) *Optimal Branch Metric for SC schemes with Impulse Noise*: Defining by $\mathbf{r} \triangleq \mathbf{r}_1^K$ the complex vector given by the sequence of samples at the output of the channel, where K is the transmission length, the MAP detection strategy can be formulated as

$$\hat{\mathbf{a}} = \operatorname{argmax}_{\mathbf{a}} p(\mathbf{r}|\mathbf{a})P\{\mathbf{a}\} \quad (8)$$

where $p(\mathbf{r}|\mathbf{a})$ is the conditional PDF of the vector \mathbf{r} given the information sequence \mathbf{a} , and $P\{\mathbf{a}\}$ is the probability of the information sequence. Since the trellis encoder can be described as a time-invariant finite state machine (FSM), it is possible to define a sequence of states $\{\mu_0, \mu_1, \dots\}$ over which the encoder evolves and define a deterministic state transition law $f(\cdot, \cdot)$ which describes the evolution of the system caused by the information sequence, i.e., $\mu_k = f(\mu_{k-1}, a_{k-1})$. As a consequence, the evolution of the FSM associated with the TCM encoder can be described through a trellis diagram, in which there is a fixed number of exiting branches from each state. This number depends on the number of subsets in which the constellation is partitioned [5]. Under these assumptions, we can write the discrete-time observable as

$$r_k = c_k(a_k, \mu_k) + w_k + i_k$$

where the TCM coded symbol $c_k(a_k, \mu_k)$, belonging to a QAM constellation, is a function of the encoder state μ_k and the information symbol a_k at the input of the coder. Assuming causality and absence of memory, discarding irrelevant terms and applying the chain factorization rule to the conditional PDF, we can rewrite (8) as

$$\begin{aligned} \hat{\mathbf{a}} &= \operatorname{argmax}_{\mathbf{a}} \prod_{k=0}^{K-1} p(r_k | \mathbf{r}_0^{k-1}, \mathbf{a}_0^k) P\{a_k\} \\ &= \operatorname{argmax}_{\mathbf{a}} \prod_{k=0}^{K-1} p(r_k | a_k, \mu_k) P\{a_k\}. \end{aligned}$$

Recalling the definition (2) for the PDF for the Bernoulli-Gaussian noise and assuming that the information symbols are independent and equally probable, the MAP sequence detection strategy can be expressed in the logarithmic domain as

$$\begin{aligned} \hat{\mathbf{a}} &= \operatorname{argmax}_{\mathbf{a}} \sum_{k=0}^{K-1} \ln \left\{ (1-p) \mathcal{N}(r_k; c_k(a_k, \mu_k), \sigma_w^2) \right. \\ &\quad \left. + p \mathcal{N}(r_k; c_k(a_k, \mu_k), \sigma_w^2 + \sigma_i^2) \right\}. \quad (9) \end{aligned}$$

Defining the quantities

$$\alpha_k(a_k, \mu_k) \triangleq \frac{1}{2\sigma_w^2} \left\{ |r_k - c_k(a_k, \mu_k)|^2 \right\} - \ln \left(\frac{1-p}{2\pi\sigma_w^2} \right)$$

$$\begin{aligned} \beta_k(a_k, \mu_k) &\triangleq \frac{1}{2(\sigma_w^2 + \sigma_i^2)} \left\{ |r_k - c_k(a_k, \mu_k)|^2 \right\} \\ &\quad - \ln \left(\frac{p}{2\pi(\sigma_w^2 + \sigma_i^2)} \right) \end{aligned}$$

one can show that (9) can be rewritten as

$$\begin{aligned} \hat{\mathbf{a}} &= \operatorname{argmin}_{\mathbf{a}} \sum_{k=0}^{K-1} \left\{ \min[\alpha_k(a_k, \mu_k), \beta_k(a_k, \mu_k)] \right. \\ &\quad \left. - \ln \left(1 + e^{-|\Delta_k(a_k, \mu_k)|} \right) \right\} \quad (10) \end{aligned}$$

where $\Delta_k(a_k, \mu_k) \triangleq \alpha_k(a_k, \mu_k) - \beta_k(a_k, \mu_k)$. The detection strategy defined in (10) can now be used to perform sequence detection in SC schemes with TCM, where the impulse noise is modeled as a Bernoulli-Gaussian process. The branch metric to be used in the Viterbi algorithm at time step k is simply defined as the k -th term of (10). We point out that a similar technique is used in [8] to compute the branch metric for a VA, considering a different impulse noise channel model. This suggests that the theoretical framework proposed in this paper can be extended straightforwardly to scenarios with different types of impulse noise.

2) *Optimal Branch Metric for Interleaved MC Schemes with Impulse Noise*: In order to derive the branch metric for an MC TCM coded system, assuming i.i.d. noise samples, we can simply adapt the detection strategy (9) using the PDF of the noise defined in (3). As a consequence, we can rewrite (9) as

$$\begin{aligned} \hat{\mathbf{a}} &= \operatorname{argmax}_{\mathbf{a}} \sum_{k=0}^{K-1} \ln \left\{ \sum_{\ell=0}^N \binom{N}{\ell} p^\ell (1-p)^{N-\ell} \right. \\ &\quad \left. \cdot \mathcal{N}(r_k; c_k(a_k, \mu_k), \sigma_M^2[\ell]) \right\} \quad (11) \end{aligned}$$

where $\sigma_M^2[\ell]$ is defined as in (4). Defining

$$\begin{aligned} \delta_k^{(\ell)}(a_k, \mu_k) &\triangleq \frac{1}{2\sigma_M^2[\ell]} \left\{ |r_k - c_k(a_k, \mu_k)|^2 \right\} \\ &\quad - \ln \left\{ \binom{N}{\ell} p^\ell (1-p)^{N-\ell} \right\} + \ln(2\pi\sigma_M^2[\ell]) \end{aligned}$$

one can express (11) as

$$\begin{aligned} \hat{\mathbf{a}} &= \operatorname{argmin}_{\mathbf{a}} \sum_{k=0}^{K-1} \left\{ \min[\delta_k^{(0)}(a_k, \mu_k), \bar{\delta}_k^{(1)}(a_k, \mu_k)] \right. \\ &\quad \left. - \ln \left(1 + e^{-|\bar{\Delta}_k^{(0)}(a_k, \mu_k)|} \right) \right\} \quad (12) \end{aligned}$$

where the quantities $\bar{\delta}_k^{(\ell)}(a_k, \mu_k)$ and $\bar{\Delta}_k^{(\ell)}(a_k, \mu_k)$ are recursively defined, for $\ell = 0, \dots, N-2$, as

$$\begin{aligned} \bar{\delta}_k^{(\ell)}(a_k, \mu_k) &= \min[\delta_k^{(\ell)}(a_k, \mu_k), \bar{\delta}_k^{(\ell+1)}(a_k, \mu_k)] \\ &\quad - \ln \left(1 + e^{-|\bar{\Delta}_k^{(\ell)}(a_k, \mu_k)|} \right) \\ \bar{\Delta}_k^{(\ell)}(a_k, \mu_k) &= \delta_k^{(\ell)}(a_k, \mu_k) - \bar{\delta}_k^{(\ell+1)}(a_k, \mu_k) \end{aligned}$$

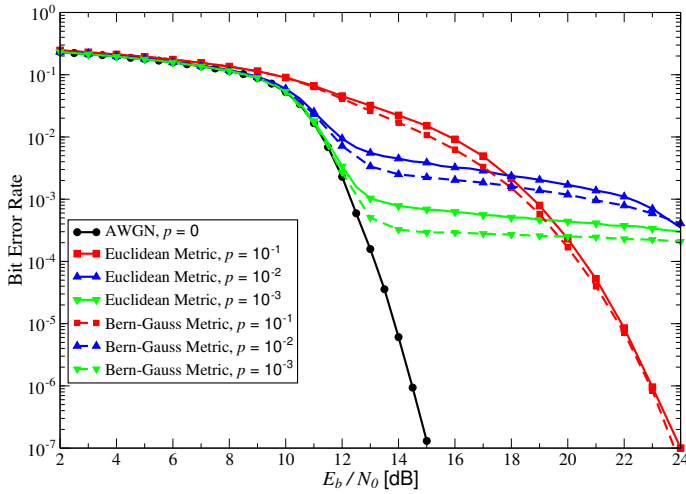


Fig. 5. Bit error rate performances, in the presence of impulse noise, for a 64 QAM TCM-4D coded SC system with Euclidean branch metric and the proposed modified branch metric.

and, for $\ell = N - 1$, as

$$\bar{\delta}_k^{(N-1)}(a_k, \mu_k) = \min[\delta_k^{(N-1)}(a_k, \mu_k), \delta_k^{(N)}(a_k, \mu_k)] - \ln \left(1 + e^{-|\Delta_k^{(N-1)}(a_k, \mu_k)|} \right)$$

with $\Delta_k^{(N-1)}(a_k, \mu_k) = \delta_k^{(N-1)}(a_k, \mu_k) - \delta_k^{(N)}(a_k, \mu_k)$.

While the above branch metrics are *exact* for an interleaved MC scheme, in the following subsection they will be used in standard (i.e., non-interleaved) MC schemes, where they are suboptimal. More precisely, the second equality in the derivation of (9) does not hold in an MC scenario, and the correct branch metric to be used would be given by $\ln p(r_k | \mathbf{r}_0^{k-1}, \mathbf{a}_0^k)$. This metric is very complicated to compute, and it is expedient to use the simpler metric calculated for an interleaved MC channel. As it will be shown in the following section, the performance obtained using the latter metric is reasonable and in agreement with the information-theoretic results. The rationale behind this behavior lies in the fact that the DFT block “spreads” the impulse noise over all symbols. Therefore, the samples of the output of this block have, more or less, a Gaussian distribution and are approximately independent. Explicit computation of the exact metric for an MC scheme is an open problem.

3) *Numerical Results:* In Fig. 5, the performance of an SC scheme with TCM is assessed in terms of BER versus the bit SNR E_b/N_0 , where E_b is the received energy per information bit and $N_0 = \sigma_w^2$ is the one-sided noise power spectral density. The considered values for p are 10^{-1} , 10^{-2} and 10^{-3} , and the considered coding scheme is an eight-state four-dimensional (4D) 64 QAM TCM scheme [9]. Two different branch metrics have been considered: the standard Euclidean branch metric, i.e., exact for AWGN channel *without* impulse noise, and the Bernoulli-Gaussian metric given by (10). The average power of the impulse noise is kept equal to the power of the AWGN, i.e., $\sigma_w^2 = p \sigma_i^2$. One can observe that, as in the case of uncoded QAM, the presence of impulse noise causes an error floor at BER values close to the Bernoulli parameter p . Moreover,

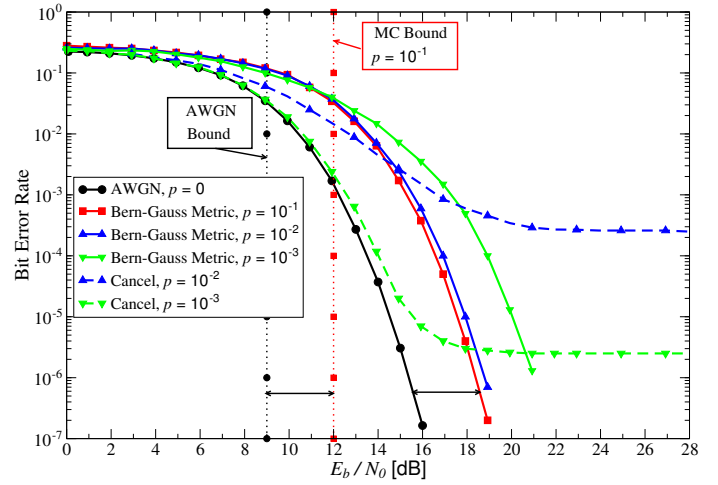


Fig. 6. Bit error rate performances, in presence of impulse noise, for a 64 QAM TCM-2D coded MC system with Euclidean branch metric and with cancellation of the sample affected by impulse noise (number of sub-channels equal to $N = 1024$).

depending on the values of the SNR and p , the use of the optimal branch metric provide a gain ranging from 0 dB to 6 dB in terms of SNR, but minor in terms of BER. In other words, these results show that in a scenario with impulse noise, TCM schemes are not suitable to cope with impulse noise. This is due to the insufficient protection of the uncoded bits, provided by “set partitioning,” against the impulse noise.

In Fig. 6, the performance of a similar MC system with the same 64 QAM TCM coding scheme is shown, the only difference with the previous case being that the number of sub-carriers is now $N = 1024$. The considered channel is the 64 kV dispersive channel proposed in [10]. The analyzed schemes are the scheme with AWGN (used as a reference model) and the scheme with Bernoulli-Gaussian impulse noise with parameter $p \in \{10^{-1}, 10^{-2}, 10^{-3}\}$. In the case with impulse noise, we first consider the use of the optimal branch metric derived in (12) and, for reference, we also show the SNR limit predicted by the information-theoretic results. Motivated by the results in Section III, we also consider the use of a simple time-domain processor before DFT demodulation. This processor simply detects the presence of noise impulses and substitutes them with zeros.² The corresponding BER curves are denoted as “Cancel.” Considering in Fig. 6 the BER curves corresponding to the system using the time-domain processor, one can conclude that a simple impulse noise cancellation algorithm can prevent almost the entire loss due to the impulse noise, as long as the occurrence frequency of the latter is sufficiently low. We remark that the error floor affecting these BER curves is due to the non-zero “false-alarm” cancellation rate. Use of impulse noise cancellation techniques is also proposed in [11].

B. LDPC-Coded Transmission

In LDPC-coded schemes, the transmitter first collects information bits into vectors of length k which are encoded by an

²Note that detection of a bit interval affected by an impulse of noise can be easily implemented by using a proper threshold detector.

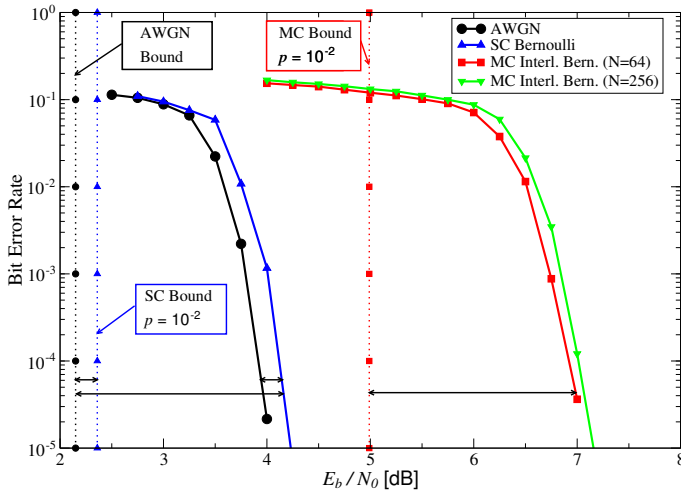


Fig. 7. Bit error rate performance, for an LDPC coded 16 QAM over AWGN channel and Bernoulli impulse noise channel both SC and interleaved MC. The LDPC code is regular (3,6), the codeword length is 6000. Bernoulli parameter $p = 10^{-2}$.

LDPC encoder into a vector of binary symbols of length n , i.e., the codeword. The LDPC codeword binary symbols are then grouped into 4-tuples and fed to the modulator which performs Gray mapping of the bits into 16-QAM symbols. At the receiver a 16-QAM soft demapper computes the a posteriori probability (APP) of each component bit of the 16-QAM symbol based on the constellation structure and the noise PDF. The APPs are fed to the LDPC decoder which decodes the codeword with the Gallager soft algorithm [6]. By exploiting the random nature of LDPC codes, it can be shown that the described scheme is a particular instance of bit interleaved coded modulation (BICM) schemes [12], where the interleaver has been omitted due to the random structure of the LDPC code. BICM allows to treat the set modulator-channel-demodulator as a memoryless channel. Since the performance of LDPC codes over memoryless channels depends almost only on the information rate of the channel [13], we expect that the performance of the proposed LDPC-coded system over the considered channels will behave as predicted by the information rate results in Fig. 4.

In Fig. 7, the performance of a regular (3,6) LDPC code [14] mapped over a 16 QAM constellation, and transmitted over the three considered channels, is shown. The codeword length is 6000. The maximum number of iterations is set to 100—if the decoder finds a codeword before the 100th iteration, it stops. The parameter of the Bernoulli-Gaussian impulse noise is $p = 10^{-2}$, and the power of the impulse noise process equals the power of the AWGN. The MC scheme makes use of a number N of carriers equal to 64 and 256, respectively. As a reference, the theoretical bounds at the corresponding spectral efficiency of 2 bits/channel use, are shown, as vertical lines, for (i) the SC scheme with AWGN, (ii) the SC scheme with impulse noise and (iii) the interleaved MC scheme with impulse noise. The performance gap, in terms of SNR, is about 0.3 dB between the SC scheme with AWGN and the SC scheme with impulse noise, whereas the gap is approximately 3 dB between the SC scheme with AWGN and the interleaved MC scheme with

impulse noise. These results are in excellent agreement with the theoretical limits predicted in Fig. 4.

V. CONCLUDING REMARKS

In this paper, the impact of impulse noise on PLC systems has been investigated. We have first analyzed the impact of impulse noise in terms of *information rate*. These theoretical results suggest that MC schemes are “intrinsically” less robust, in terms of power and spectral efficiency, to impulse noise than SC schemes. In order to validate these theoretical conclusions, we have evaluated the BER performance of several coded-modulated schemes (both with TCM and with LDPC-coded modulations), confirming the theoretical predictions. Our conclusion is that MC schemes can be effective *only* if proper signal processing techniques are used—a simple cancellation technique has been considered in this work. While in this paper we have adopted a simplified model for both the impulse noise and the channel frequency response in the information rate analysis, the qualitative implications are quite general, and we believe that they should be taken into careful account in modern high-efficiency system design for systems impaired by impulse noise. The extension of the proposed theoretical analysis to a more realistic PLC channel model, characterized by the presence of inter-symbol interference and colored noise, will be object of further investigations.

REFERENCES

- [1] H. C. Ferreira, “Power line communications: an overview,” in *Proc. IEEE 4th AFRICON*, vol. 2, Stellen-Bosch, South Africa, Sept. 1996, pp.558-563.
- [2] E. Biglieri, “Coding and modulation for a horrible channel,” *IEEE Commun. Mag.*, vol. 41, no. 5, pp. 92–98, May 2003.
- [3] M. Ghosh, “Analysis of the effect of impulsive noise on multicarrier and single-carrier QAM systems,” *IEEE Trans. Commun.*, vol. 44, no. 2, pp. 145–147, February 1996.
- [4] T. M. Cover and J. A. Thomas, *Elements of Information Theory*. New York: John Wiley & Sons, 1991.
- [5] G. Ungerboeck, “Channel coding with multilevel/phase signals,” *IEEE Trans. Inform. Theory*, vol. 28, pp. 55–67, January 1982.
- [6] R. G. Gallager, *Low-Density Parity-Check Codes*. Cambridge, MA: MIT Press, 1963.
- [7] D. Arnold, H. A. Loeliger, P. O. Vontobel, A. Kavcic, and W. Zen, “Simulation-based computation of information rates for channel with memory,” January 2004, available at <http://hrl.harvard.edu/~kavcic/recent.html>.
- [8] S. Miyamoto, M. Katayama, and N. Morinaga, “Optimum detection and design of TCM signals under impulsive noise environment,” in *Systems Engineering, 1992., IEEE International Conference on*, September 1992, pp. 473–478.
- [9] L. F. Wei, “Trellis coded modulation with multidimensional constellation,” *IEEE Trans. Commun.*, vol. IT-33, no. 4, pp. 483–501, July 1987.
- [10] R. Pighi and R. Raheli, “On multicarrier signal transmission for high-voltage power lines,” in *Proc. Int. Symp. Power-Line Commun. and Its Apps.*, Vancouver, Canada, April 2005.
- [11] F. Abdelkefi, P. Duhamel, and F. Alberge, “Impulse noise cancellation in multicarrier transmission,” *IEEE Trans. Commun.*, vol. 53, no. 1, pp. 94–106, January 2005.
- [12] G. Caire, G. Taricco, and E. Biglieri, “Bit-interleaved coded modulation,” *IEEE Trans. Inform. Theory*, vol. 44, no. 3, pp. 927–946, May 1998.
- [13] M. Franceschini, G. Ferrari, and R. Raheli, “Does the performance of LDPC codes depend on the channel?” in *Proc. Int. Symp. Inform. Theory and Applic. (ISITA'04)*, Parma, Italy, October 2004.
- [14] T. Richardson and R. Urbanke, “The capacity of low density parity check codes under message passing decoding,” *IEEE Trans. Inform. Theory*, vol. 47, pp. 599–618, February 2001.